attenuate the magnitude of the reflection coefficient at distance points not equal to the electrical location, shown in Fig. 2.

The characteristics of the slot, Fig. 3(a) and (b), were impedance matched according to (1) by a dielectric post. The relative dielectric constant of 4.07 was used to characterize the post [3]. The results of the optimized impedance match using the dielectric post are given in Fig. 4. The calculated physical parameters of this dielectric post are as follows: diameter: 0.297 cm; sidewall distance: 0.477 cm; distance from center of slot 1.705 cm toward the load.

In order to improve the impedance match of the slot and dielectric post, the resulting complex reflection coefficient was again used as a discontinuity in the matching computer program. During this iterative calculation a capacitive iris was the matching element for the resultant mismatch of slot and dielectric post. The result of this effort is shown in Fig. 5. The symmetrical capacitive iris with thickness 0.035 cm and height 0.06 cm was located 0.7 cm toward the generator from the *electrical* location of the slot. The dielectric post was located 0.312 cm toward the load from the *electrical* location of the slot.

Boron nitride was machined into a post with a diameter of 0.117 ± 0.002 in and inserted between the walls of the waveguide to the position given in Fig. 5. The final location of the dielectric post was within 0.002 in of the calculated location. The symmetical capacitive iris was machined to fit two slots sawed through the broad wall of the waveguide. The slots were 0.014 ± 0.002 in wide and 0.074 ± 0.002 in deep. The dielectric post was positioned in the guide, and the capacitive irises were fitted into the respective slots. A silver-based conductive paint was painted on the outside wall of the waveguide over the ends of the irises and on the intersection of the iris and the inside waveguide walls.

The impedanced matched shunt slot radiator was then measured by the slotted line at 100-MHz intervals from 8.575 to 10.875 GHz. The results of these measurements, seen in Fig. 6, show excellent agreement between the computer calculated VSWR and the experimentally measured VSWR.

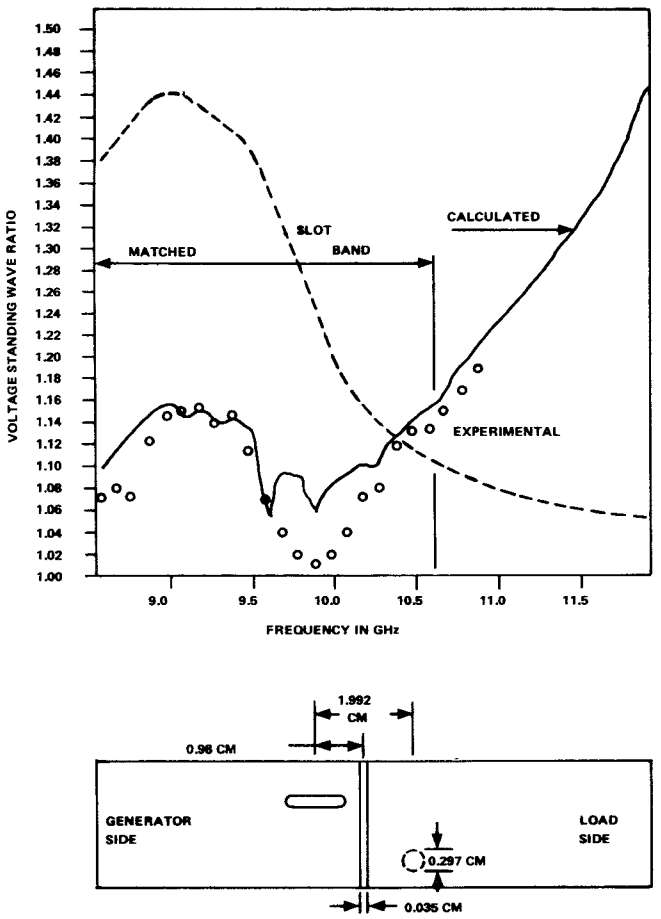

Fig. 6. Comparison of calculated mismatch and measured mismatch.

CONCLUSIONS

The combined use of the comparison reflectometer and the computational procedure developed in this study makes it possible to resolve individual sources of reflections in a waveguide and to synthesize waveguide obstacles that are capable of matching the original discontinuity. The computational time required is short (approximately 100 s on a Univac 1108) and the output includes both the parameters of the matching structure and the expected final performance. Experimental verification of the technique corroborates the theory. Due to approximations in the theory at its present state of development, its application is limited to original discontinuities having VSWR's less than approximately 1.5.

REFERENCES

[1] D. L. Hollway, "The comparison reflectometer," *IEEE Trans. Microwave Theory Tech.*, vol. MTT-15, pp. 250–259, Apr. 1967.
[2] R. S. Gordy, "A computer aided broad band impedance matching technique using a comparison reflectometer." Ph.D. dissertation, Georgia Inst. Technol., Altanta, July 1972.
[3] N. Marcuvitz, *Waveguide Handbook*. New York: Dover, 1965.

Modal Characteristics of Quadruple-Ridged Circular and Square Waveguides

M. H. CHEN, MEMBER, IEEE, G. N. TSANDOULAS, MEMBER, IEEE, AND F. G. WILLWERTH

***Abstract*—A theoretical study, backed by experimental verification, was undertaken to determine the modal characteristics of quadruple-ridged circular and square waveguides. Field lines for the first few important modes and cutoff frequencies were determined. It is shown that for square waveguides quadruple-ridge loading always decreases the TE_{10}–TE_{11} bandwidth whereas for circular waveguides only a small amount of additional separation between the first two fundamental modes may be obtained over a limited parameter range. Symmetrical excitation will not excite the asymmetrical higher-order modes. This feature makes these waveguides acceptable as feeds for wide-band reflector antennas and for similar applications but raises a question mark regarding their use as radiators in wide-band phases arrays.**

I. INTRODUCTION

Phased array antennas operating in the *L*-band or higher frequency regions, commonly use waveguide radiating elements. To provide dual-polarization capability, it is natural to use circular or square waveguides as radiators because they can support two orthogonal modes [1].

Based on the cutoffs of the first two (TE_{10},TE_{11}) waveguide modes, maximum available bandwidth for square waveguides is about 34 percent of center frequency [1]. For circular waveguides the TE_{11}–TM_{01} bandwidth is only about 26.5 percent of center frequency. Thus circular waveguides compare unfavorably with square waveguides as far as maximum bandwidth is concerned. The first higher order mode limitation on bandwidth has been shown to be valid in order to avoid mode resonance effects that may give blind spots in the array scan pattern [1], [2].

In many phased array applications, the circular radiator shape is advantageous for symmetry and other reasons. If bandwidths much in excess of about 17 percent (maximum bandwidth reduced by about 10 percent to allow good matching to the exciter at the low end of the frequency band) are required, some way of increasing the available bandwidth is desirable. It has been known that ridged rectangular waveguides exhibit greatly enhanced bandwidth [3].

Manuscript received October 20, 1973; revised January 17, 1974. This work was sponsored by the Department of the Army.
M. H. Chen was with the Massachusetts Institute of Technology, Lincoln Laboratory, Lexington, Mass. 02173. He is now with COMSAT, Clarksburg, Md.
G. N. Tsandoulas and F. G. Willwerth are with the Massachusetts Institute of Technology, Lincoln Laboratory, Lexington, Mass. 02173.

The quadruple-ridged circular guide[1] has also been commonly considered as a very wide-band radiator, until now. The following theoretical and experimental investigation, however, shows that only a limited increase in bandwidth may be available and then only if the design parameters are properly chosen. A previous investigation [4] has identified the bandwidth-determining TM_{01} mode experimentally by symmetrical excitation of the quadruple-ridged circular guide. However, if asymmetrical excitation is applied, the next higher mode, the TE_{21}, propagates and supersedes the TM_{01}. In the resulting modal inversion the TE_{21} mode is heavily loaded by the ridges and so its cutoff point is lowered, reducing bandwidth.

This phenomenon is particularly important in phased arrays in which off-boresight scanning is equivalent to asymmetrical excitation with the concomitant entrance of the TE_{21} mode in the excited or near-cutoff waveguide modal spectrum which may give rise to blind spots.

II. COMPUTATIONAL METHOD

The analytical study is performed with a computer program that calculates the eigenvalues and scalar potentials for an arbitrarily shaped waveguide. The analysis was developed by Konrad and Sylvester using the triangular-finite-element method [5]. The program solves the scalar two-dimensional Helmholtz equation

$$(\nabla^2 + k_c^2)\Phi(x,y) = 0 \tag{1}$$

subject to proper boundary conditions. Since the scalar potential represents either the longitudinal magnetic field H_z for the TE modes or the longitudinal electric field E_z for the TM modes, the boundary conditions for these modes are, respectively, $\partial\Phi/\partial n = 0$ and $\Phi = 0$. The solutions of (1) are eigenvalues k_{c_i} and eigenfunctions $\Phi_i(x,y)$. The k_{c_i} may be related to the modal cutoff frequency and the $\Phi_i(x,y)$ may be related to the field distribution for mode i in the waveguide.

The geometry of the waveguide is defined by the straight lines that connect two points with a special code specified as the "boundary line." Since straight-line boundaries are required by the program, the circular waveguide was simulated by a 16-sided polygon. To verify the validity of this representation, a 32-sided polygon was also computed. The difference in cutoff frequencies was less than 1 percent. It was decided that this was too small to warrant the considerably longer computation times required for the 32-sided-polygon representation.

Because of symmetry (Fig. 1), the double-bisection method was used. Thus only one quarter of the cross-sectional area needs to be computed. For each quarter-section, the following parameters were used in the numerical procedure:

number of triangles	6 (square)
	8 (circular)
order of each triangle	5 (square)
	4 (circular)
total points computed	96 (square)
	85 (circular).

III. MODAL CUTOFFS AND BANDWIDTH PROPERTIES

The solutions of (1) represent distinct waveguide modes for the specified waveguide. The cutoff wavelength λ_{c_i} for mode i can be computed from the eigenvalue k_{c_i} by

$$\lambda_{c_i} = \frac{2\pi}{k_{c_i}}, \qquad i = 1,2\cdots. \tag{2}$$

The percent bandwidth BW of the specified waveguide is computed from the relation

$$\text{BW} = \frac{\lambda_{c-} - \lambda_{c+}}{\lambda_{c-} + \lambda_{c+}} \times 200 \text{ percent} \tag{3}$$

where λ_{c-} is the cutoff wavelength for the fundamental mode, and λ_{c+} is the cutoff wavelength for the first higher order mode. The value of BW thus obtained is as a percentage of the center frequency between the two modal cutoffs.

[1] This type of waveguide has been used as a radiator in phased arrays in which an empty guide would be too large to fit within the lattice dimensions.

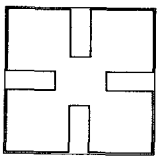

QUADRUPLE-RIDGED SQUARE WAVEGUIDE

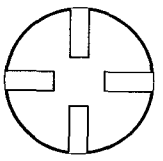

QUADRUPLE-RIDGED CIRCULAR WAVEGUIDE

Fig. 1. Transverse geometry of quadruple-ridged square and circular waveguides.

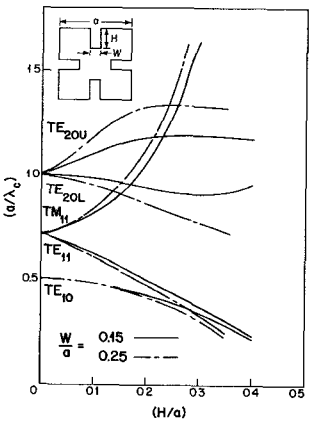

Fig. 2. Modal cutoff frequencies of quadruple-ridged square waveguide

A. Quadruple-Ridged Square Waveguide

The modal cutoff frequencies for quadruple-ridged square waveguide with various ridge widths and heights have been computed and plotted (Fig. 2). Ridge loading lowers the cutoff frequencies for the TE_{10} and TE_{11} modes, raises the cutoff frequency of the TM_{11} mode, and splits the TE_{20} mode, lifting an orthogonal degeneracy. This mode-splitting phenomenon occurs because the ridges load differently the two diagonal modes obtained by the sum and difference of the two orthogonal TE_{20} modes (capacitively for one branch, inductively for the other). Because the ridges represent a heavier load for the TE_{11} mode than for the TE_{10}, the bandwidth decreases monotonically. By contrast, in a rectangular waveguide ridge loading lowers the TE_{10} mode cutoff but has only a small effect on the TE_{20} mode cutoff resulting in a bandwidth increase with ridge height.

The bandwidth characteristics for quadruple-ridged square waveguides have been computed according to the definition of (3) and plotted in Fig. 3. Maximum bandwidth occurs when ridge height is zero, which represents an ordinary square waveguide without ridges. Therefore, quadruple-ridge loading in a square waveguide does not broaden the bandwidth.

B. Quadruple-Ridged Circular Waveguide

In quadruple-ridged circular waveguide, ridge loading lowers the cutoff frequency of the TE_{11} mode, raises the cutoff frequency of the TM_{01} mode, and splits the TE_{21} mode (Fig. 4). This mode-splitting phenomenon is similar to that for the TE_{20} mode in square waveguides. Also in both cases, ridge width has much less influence on the cutoff frequencies than does ridge height.

In the bandwidth curves for quadruple-ridged circular waveguide (Fig. 5), to the left of the peaks, bandwidth is determined by the TE_{11}

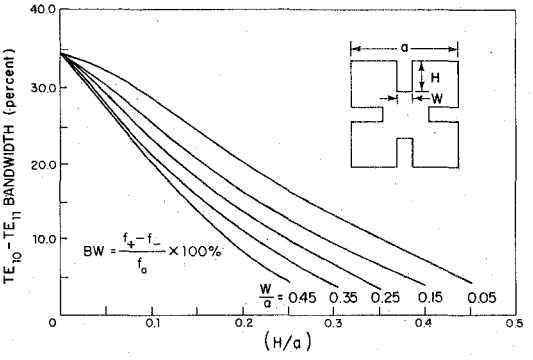

Fig. 3. Bandwidth dependence curves of quadruple-ridged square waveguide.

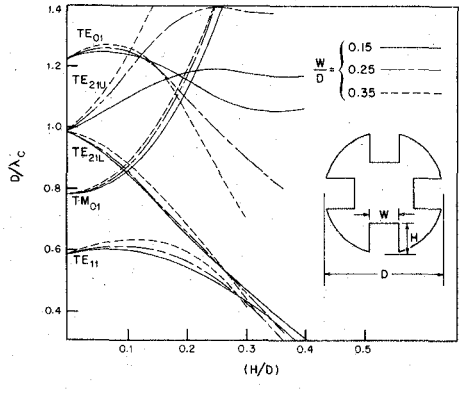

Fig. 4. Modal cutoff frequencies of quadruple-ridged circular waveguide.

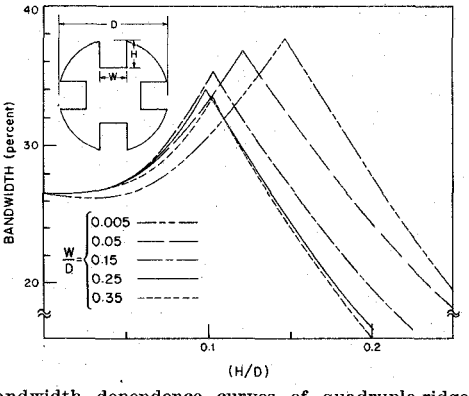

Fig. 5. Bandwidth dependence curves of quadruple-ridged circular waveguide.

and TM_{01} modes, while to the right by the TE_{11} and TE_{21} modes. It is interesting to note that dielectric-lined circular waveguide also exhibits a bandwidth maximum but not directly related to the TE_{21} mode cutoff [6]. Although ridge width does not affect the modal cutoff frequencies very much, it is important in determining maximum bandwidth (about 38 percent). It is seen that the introduction of very small ridges in circular waveguides makes them equivalent to empty square waveguides as far as bandwidth is concerned. Because of the small ridge size, existing analytical techniques for circular waveguide arrays may in all likelihood still be valid in predicting mutual coupling performance.

IV. FIELD DISTRIBUTIONS

The transverse field distribution for quadruple-ridged square and circular waveguides can be obtained from the computed scalar potential $\Phi(x,y)$. The scalar potential represents the longitudinal component of the magnetic field for TE modes and of the electric field for TM modes. Therefore, the transverse electric and magnetic

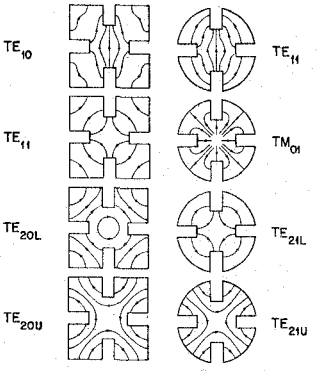

Fig. 6. Field distribution of quadruple-ridged square and circular waveguide.

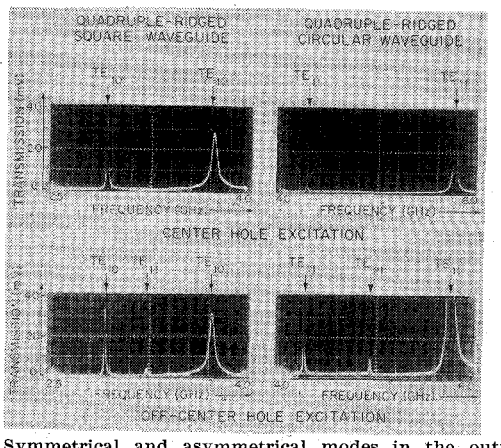

Fig. 7. Symmetrical and asymmetrical modes in the output of a transmission swept measurement.

fields can be derived from [7]

$$\left.\begin{aligned} \boldsymbol{H}_t(x,y) &\sim \nabla_t \Phi_{\mathrm{TE}}(x,y) \\ \boldsymbol{E}_t(x,y) &\sim \hat{z}_0 \boldsymbol{x} \nabla_t \Phi_{\mathrm{TE}}(x,y) \end{aligned}\right\} \text{TE modes}$$

$$\left.\begin{aligned} \bar{E}_t(x,y) &\sim \nabla_t \Phi_{\mathrm{TM}}(x,y) \\ \bar{H}_t(x,y) &\sim \hat{z}_0 \boldsymbol{x} \nabla_t \Phi_{\mathrm{TM}}(x,y) \end{aligned}\right\} \text{TM modes.} \qquad (4)$$

Accordingly, the equipotential lines represent electric field lines for the TE modes and magnetic field lines for the TM modes.

Fig. 6 shows the field patterns for the dominant mode as well as for a few higher order modes for quadruple-ridged square and circular waveguides. In a metallic-obstacle-loaded waveguide, when an electric field points toward the obstacle, capacitive loading results. When the field points around the obstacle, the loading is inductive. Therefore, the ridges for the TE_{20L} mode and the TE_{21L} mode are capacitances and the ridges for the TE_{20U} mode and the TE_{21U} mode are inductances.

The field patterns shown are not simply conceptual drawings but were determined using a limited number of computer-provided points. Complete calculations would require rather large amounts of computer time.

V. EXPERIMENTAL STUDY

The experimental study is based on transmission cavity measurements. The cavity is a section of quadruple-ridged square (or circular) waveguide and two shorting plates with coupling holes. The output is the transmission characteristic of the cavity shown on the oscilloscope, where the horizontal axis is frequency and the vertical axis is transmitted voltage (Fig. 7). The peaks indicate where the cavity resonances occur along the frequency axis. The cutoff frequency of the waveguide may be computed from the resonant frequency of the cavity.

The transverse field distributions of quadruple-ridged square and circular waveguides (Fig. 6) show that the center coupling hole

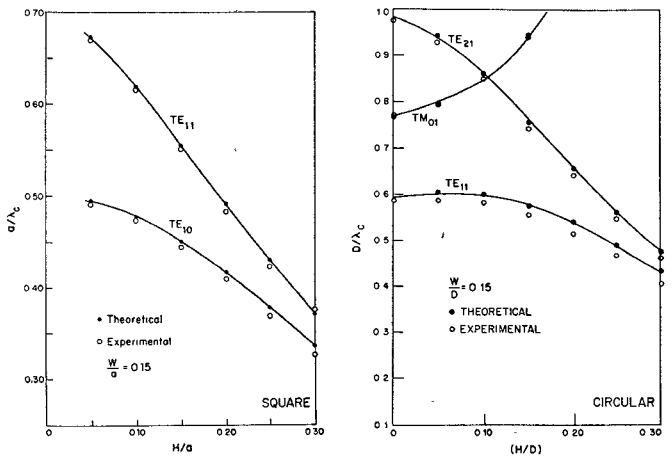

Fig. 8. Experimental versus computed modal cutoff frequencies for quadruple-ridged circular and square waveguide.

only excites the TE_{10} mode in a square waveguide and the TE_{11} mode in a circular waveguide, because all of the other modes shown have a null field at the center. When the coupling hole is moved to a corner, all the modes are excited. Typical outputs of a transmission sweep measurement for quadruple-ridged square and circular waveguide with center-hole and off-center-hole excitation are given in Fig. 7. The cavity length is such that there exist two fundamental-mode resonances in the frequency range of 2.5–4.0 GHz.

The relative amplitudes of the mode resonances depend upon the location of the coupling hole. The asymmetrical modes are difficult to excite because their coupling coefficients are small compared to those of the symmetrical modes. The photographs for off-center-hole excitation show that the asymmetric mode amplitude is considerably smaller than that of the symmetrical mode. Therefore, it becomes easy to overlook some modes in an experimental study without *a priori* theoretical knowledge of their characteristics. We suspect that this is the reason why some of the published literature on the subject does not contain an accurate description of the modal spectrum. A recent paper [8] states that experimental results obtained by Clark [9] in 1971 agree with our results. However, the figure presented in support of this statement shows increasingly larger disagreement in the TE_{21L} cutoff for H/D values greater than about 0.15 to the effect that a 2:1 bandwidth is eventually reached. Our results show this limiting bandwidth to be almost zero. The error in Clark's work could be due to confusing the TE_{21L} mode with the TE_{01} mode (see Fig. 4 above), especially if the ridge width was large.

The theoretical and measured cutoff frequencies for the TE_{10} and TE_{11} modes for quadruple-ridged square waveguide, and for the TE_{11}, TM_{01}, and TE_{21} modes for quadruple-ridged circular waveguide are plotted in Fig. 8. The small circles, representing measured values, and the solid lines, representing computed values, indicate excellent agreement between theory and experiment.

VI. CONCLUSION

It is concluded from this study that quadruple-ridge loading does not broaden the bandwidth of square waveguides and only moderately broadens the bandwidth of circular waveguides because the higher order modes are heavily affected by the ridge loading.

However, the fundamental mode is a symmetrical mode, and the next higher order mode is an asymmetrical mode. The asymmetrical mode may not be excited for some applications, for example, when the waveguide is used as a feed in a reflector antenna system. Then, TM_{01}-limited octave bandwidths may be obtained, as in fact was shown to be the case [4]. But in phased array antenna applications asymmetrical modes may be excited when the beam scans off-boresight and care should be taken to guard against possible mode resonance coupling phenomena such as blind spots.

REFERENCES

[1] G. N. Tsandoulas and G. H. Knittel, "The analysis and design of dual-polarization square-waveguide phased arrays," *IEEE Trans. Antennas Propagat.*, vol. AP-21 pp. 796–808, Nov. 1973.
[2] G. H. Knittel, "The relation of blindness in phased arrays to higher mode cutoff conditions," in *1971 IEEE G-AP Int. Symp. Dig.*, Sept. 1971, p. 69.
[3] S. Hopfer, "The design of ridged waveguides," *IRE Trans. Microwave Theory Tech.*, vol. MTT-3, pp. 20–29, Oct. 1955.
[4] J. K. Shimizu, "Octave bandwidth feed horn for paraboloid," *IRE Trans. Antennas Progagat.*, pp. 223–224, Mar. 1961.
[5] A. Konrad and P. Sylvester, "Scalar finite-element program package for two-dimensional field problems," *IEEE Trans. Microwave Theory Tech. (1971 Symposium Issue)*, vol. MTT-19, pp. 952–954, Dec. 1971.
[6] G. N. Tsandoulas, "Bandwidth enhancement in dielectric-lined circular waveguide," *IEEE Trans. Microwave Theory Tech.*, vol. MTT-21, pp. 651–654, Oct. 1973.
[7] R. E. Collin, *Field Theory of Guided Waves*. New York: McGraw-Hill, 1966.
[8] C. C. Chen, "Quadruple ridge-loaded circular waveguide phased arrays," *IEEE Trans. Antennas Propagat.* (Succinct Papers), vol. AP-22, pp. 481–483, May 1974.
[9] R. T. Clark, Ridge loaded circular guide," Hughes Aircraft Co., IDC Ref. 71/1422.00-54, Oct. 1971.

Experimental Study of Series Connected TRAPATT Diodes

K. REED GLEASON, MEMBER, IEEE, C. T. RUCKER, MEMBER, IEEE, N. W. COX, MEMBER, IEEE, A. C. MACPHERSON, SENIOR MEMBER, IEEE, AND ELIOT D. COHEN, MEMBER, IEEE

***Abstract*—The results of experiments using TRAPATT diodes connected in series at 0.5, 2, and 8 GHz are described. These experiments demonstrate that successful series operation of TRAPATT's at frequencies up to at least 2 GHz can be achieved in a configuration suitable for long pulsewidth or CW operation. An 8-GHz operation of series stacked TRAPATT's yielded high power outputs at the same efficiency achieved with single devices but no well heat sunk configuration was found that yielded good efficiency.**

INTRODUCTION

The series connection of TRAPATT diodes is a desirable way to obtain increased power output over that afforded by a single device, particularly because this connection results in an increased impedance level. In the past, TRAPATT diodes have been operated in series-stack configurations at *D* and *E* bands to generate high peak power outputs with good efficiency [1], [2]. Stacking is attractive because parasitic elements which interfere with TRAPATT operation are minimized. Unfortunately, long pulsewidth and/or CW operation are difficult to achieve with this arrangement because of problems associated with heat sinking of the upper diodes in the stack. In the experiments described here other configurations were used to demonstrate that successful series operation of TRAPATT's can be achieved even with substantial parasitic capacitance and/or inductance present.

SERIES CONNECTION AT 0.5 GHZ

Two- and three-diode series connections of Fairchild FD-300 diodes were operated in the TRAPATT mode at approximately 500 MHz. These diodes are mounted in glass packages with pigtail leads. In the experiments, the series connection was made by simply soldering the leads together. The resulting interconnecting leads were approximately 165 mils long and 40 mils in diameter. The diodes were mounted in a modified GR 874-X insertion unit at one end of a conventional 14-mm diameter three-slug tuner.

Best results are summarized in Table I. In general, the series connected diodes gave better performance at higher currents than the single diodes. Note that at 1.8 A the 1,6 pair performed better than would be expected from scaling considerations; the efficiency doubled and the power increased by a factor of almost 6. The 9, 11, 12 triplet yielded 50 percent more than the sum of the powers at slightly re-

Manuscript received November 14, 1973; revised February 14, 1974. This work was supported by the Naval Electronics Systems Command under Contract N00039-72-C-0207.
K. R. Gleason, A. C. Macpherson, and E. D. Cohen are with the Naval Research Laboratory, Washington, D. C. 20375.
C. T. Rucker and N. W. Cox were with Sperry Microwave Components, Gainesville, Fla. 32601. They are now with the Engineering Experiment Station, Georgia Institute of Technology, Atlanta, Ga. 30332.